A new method for investigating infrared spectra of protonated benzene (C6H7 +) and cyclohexadienyl radical (c-C6H7) using para-hydrogen

Mohammed Bahou, Yu-Jong Wu, and Yuan-Pern Lee

Citation: The Journal of Chemical Physics **136**, 154304 (2012); doi: 10.1063/1.3703502
View online: http://dx.doi.org/10.1063/1.3703502
View Table of Contents: http://scitation.aip.org/content/aip/journal/jcp/136/15?ver=pdfcov
Published by the AIP Publishing

A new method for investigating infrared spectra of protonated benzene ($C_6H_7^+$) and cyclohexadienyl radical (*c*-C_6H_7) using *para*-hydrogen

Mohammed Bahou,[1] Yu-Jong Wu,[2,a)] and Yuan-Pern Lee[1,3,a)]
[1]*Department of Applied Chemistry and Institute of Molecular Science, National Chiao Tung University, 1001, Ta-Hsueh Road, Hsinchu 30010, Taiwan*
[2]*National Synchrotron Radiation Research Center, 101, Hsin-Ann Road, Hsinchu 30076, Taiwan*
[3]*Institute of Atomic and Molecular Sciences, Academia Sinica, Taipei 10617, Taiwan*

(Received 21 February 2012; accepted 28 March 2012; published online 17 April 2012)

We use protonated benzene ($C_6H_7^+$) and cyclohexadienyl radical (*c*-C_6H_7) to demonstrate a new method that has some advantages over other methods currently used. $C_6H_7^+$ and *c*-C_6H_7 were produced on electron bombardment of a mixture of benzene (C_6H_6) and *para*-hydrogen during deposition onto a target at 3.2 K. Infrared (IR) absorption lines of $C_6H_7^+$ decreased in intensity when the matrix was irradiated at 365 nm or maintained in the dark for an extended period, whereas those of *c*-C_6H_7 increased in intensity. Observed vibrational wavenumbers, relative IR intensities, and deuterium isotopic shifts agree with those predicted theoretically. This method, providing a wide spectral coverage with narrow lines and accurate relative IR intensities, can be applied to larger protonated polyaromatic hydrocarbons and their neutral species which are difficult to study with other methods.
 [http://dx.doi.org/10.1063/1.3703502]

I. INTRODUCTION

Protonated aromatic hydrocarbon molecules are of fundamental importance to organic chemistry as their existence has been proposed in diverse reactions. They are widely accepted as important intermediates (Wheland intermediate) in electrophilic aromatic substitution reactions.[1] Protonated polycyclic aromatic hydrocarbons (PAH) are also postulated to be the carriers of the unidentified infrared emission (UIE) bands observed in various interstellar media.[2] In addition, the effect of protonation on aromatic biomolecules is an interesting issue for models rationalizing the ultraviolet (UV) photostability of biological molecules such as proteins and DNA.[3,4]

Protonated benzene ($C_6H_7^+$), the simplest protonated aromatic hydrocarbon, might exist as three conformers: the σ-complex **(1)**, the bridged π-complex **(2)**, and the face-centered π-complex **(3)**, as shown in Fig. 1. NMR spectra of $C_6H_7^+$ in superacid indicate that the most stable conformer of $C_6H_7^+$ at low temperature is the σ-complex **(1)** having a C_{2v} planar structure.[5–8] The experimental proton affinity of C_6H_6 fits well with the theoretical value for the formation of **(1)**, supporting that $C_6H_7^+$ exists as a σ-complex.[9–12] Quantum-chemical computations also support this assignment and predict that the bridged π-complex **(2)** is a transition state for a 1,2-H shift within **(1)** and that the face-centered π complex **(3)** is a second-order saddle point.[13,14]

Early low resolution UV (Refs. 15 and 16) and infrared (IR) (Refs. 17 and 18) spectral data of $C_6H_7^+$ isolated in superacid solutions or matrices were perturbed by the acid. The electronic absorption due to the transition $A\ ^1B_2 \leftarrow X\ ^1A_1$ of $C_6H_7^+$ in solid Ne was reported near 325 nm.[19] For IR spectra of gaseous $C_6H_7^+$, two methods have been employed. Solcà and Dopfer employed IR photodissociation (IRPD) and mass-selected ion detection to record the IR absorption in the C–H stretching region of $C_6H_7^+$ tagged with inert ligands such as Ar, N_2, CH_4, and H_2O.[20,21] Jones *et al.* produced and stored $C_6H_7^+$ in an ion-cyclotron-resonance ion trap to obtain its IR multiphoton dissociation (IRMPD) spectra using a free-electron laser and reported IR features of $C_6H_7^+$ at 1228 and 1433 cm^{-1},[22] as shown in Fig. 2(a). Douberly *et al.* recorded the IRPD spectrum of the Ar-tagged $C_6H_7^+$ complex ($C_6H_7^+$-Ar) in the spectral region 750−3400 cm^{-1} with numerous additional IR features,[23] as shown in Fig. 2(b). The bands observed with IRMPD (Ref. 22) are much broader than those recorded with IRPD and the positions are redshifted because of the anharmonic effect in multiphoton absorption. The IR spectrum of $C_6H_7^+$-Ar is expected to be similar to that of $C_6H_7^+$ because of the weak interaction between $C_6H_7^+$ and the ligands. The wavenumbers observed for $C_6H_7^+$-Ar with IRPD are in satisfactory agreement with those calculated quantum-chemically for $C_6H_7^+$,[23,24] as compared in Fig. 2(c), but the observed intensities in the C−H stretching region are much greater than predicted. This is partly because the reported spectrum is an action spectrum recorded by monitoring the intensity of $C_6H_7^+$ on tuning the wavelength of the IR laser and the observed intensity was not scaled with the IR laser power, which increases with laser wavenumber in the region 800−3200 cm^{-1}. Furthermore, the photodissociation efficiency for $C_6H_7^+$-Ar to form $C_6H_7^+$ and Ar is expected to increase with the IR excitation energy. Hence the reported action spectrum for dissociation of $C_6H_7^+$-Ar shows features in the C−H stretching region with intensities much more enhanced than those from theoretical predictions.[23]

Neutralization of $C_6H_7^+$ produces the cyclohexadienyl radical (*c*-C_6H_7) and its isomers.[19] The *c*-C_6H_7 radical is an important intermediate in the initial step in the hydrogenation of aromatic compounds in both the gaseous phase and

a)Authors to whom correspondence should be addressed. Electronic addresses: yjwu@nsrrc.org.tw and yplee@mail.nctu.edu.tw.

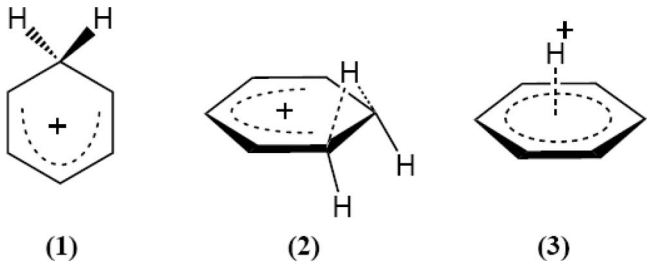

FIG. 1. Possible structures of protonated benzene. (1) σ-complex, (2) bridged π-complex, and (3) face-centered π-complex.

the condensed phase. The UV-visible spectra of c-C_6H_7 have been studied in the condensed phase[25–30] and in the gaseous phase.[31–33] The dispersed laser-induced fluorescence spectra of c-C_6H_7 radical, produced via H-abstraction of 1, 4-cyclohexadiene by Cl atom, yield wavenumbers for six vibrational modes of the ground electronic state.[34] However, except for the ν_{10} mode near 981 cm^{-1}, these modes do not match with those identified for c-C_6H_7 according to IR absorption lines of a C_6H_6/Xe matrix that was irradiated by fast electrons followed by annealing at 45 K.[35] Hence, it is important to obtain an IR spectrum of C_6H_7 with improved signal-to-noise ratio and spectral resolution.

The quantum solid *para*-hydrogen (p-H_2) has emerged as a unique host for matrix isolation spectroscopy.[36–38] The extremely narrow spectral width and a diminished matrix cage effect are some of the unique properties of the p-H_2 matrix. We have demonstrated that free radicals that are difficult to be produced via photolysis *in situ* or photo-induced bimolecular reactions using conventional noble-gas matrices can be readily produced in a p-H_2 matrix.[39–41] Here we report a new application of p-H_2 matrix isolation technique to produce protonated aromatic hydrocarbons and their neutral species. We use the IR spectra of $C_6H_7^+$ and c-C_6H_7 to demonstrate the advantages of this method.

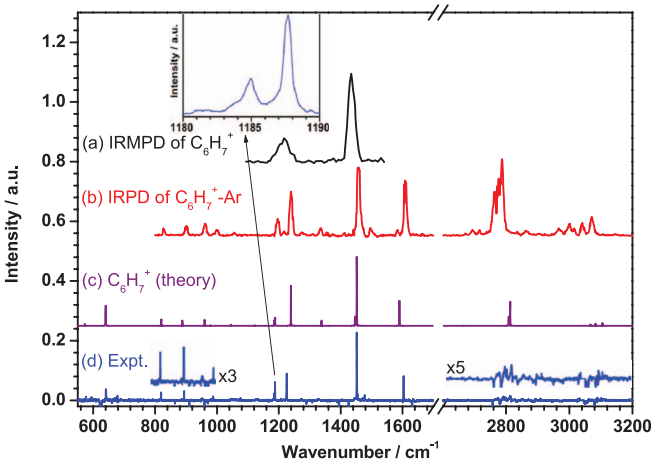

FIG. 2. Comparison of IR spectra obtained on (a) IR multiphoton dissociation of $C_6H_7^+$ (Ref. 22), (b) IR photodissociation of $C_6H_7^+$-Ar (Ref. 23), (c) theoretical prediction for $C_6H_7^+$ based on harmonic vibrational wavenumbers calculated with the CCSD(T*)-F12a/VDZ-F12 method and anharmonic contributions and IR intensities calculated with the B2PLYP-D/VTZ method,[24] and (d) IR absorption of C_6H_6/p-H_2 (1/1000) matrix sample with electron bombardment during deposition; lines due to C_6H_6 and c-C_6H_7 are stripped.

II. EXPERIMENTAL

In our experiments, a gold-plated copper plate cooled to 3.2 K served as both a cold substrate for the matrix sample and a mirror to reflect the incident IR beam to the detector.[42,43] The cooling of the substrate was achieved with a Janis RDK-415 closed-cycle helium cryostat system. IR absorption spectra were recorded with a Fourier-transform infrared spectrometer (Bomem, DA8) equipped with a KBr beamsplitter and a Hg-Cd-Te detector (cooled to 77 K) to cover the spectral range 450−5000 cm^{-1}. Six hundred scans at a resolution of 0.25 cm^{-1} were generally recorded at each stage of the experiment.

The $C_6H_7^+$ cation is produced by electron bombardment of a gaseous sample of p-H_2 containing a small proportion of C_6H_6 during deposition. Typically, a gaseous mixture of C_6H_6/p-H_2 (1/1000–1/3000, 1.3 mmol h^{-1}) was deposited over a period of 3−5 h. An electron gun (Kimball Physics, Model EFG-7) was used to generate an electron beam with energy of 250 eV and beam current of 70 μA during the deposition period. The following mechanism for the production of $C_6H_7^+$ with an excess of p-H_2 was proposed.[20]

$$H_2 + e^- \rightarrow H_2^+ + 2e^-, \tag{1}$$

$$H_2^+ + H_2 \rightarrow H_3^+ + H \qquad \Delta H = -36.0\,\text{kcal mol}^{-1}, \tag{2}$$

$$C_6H_6 + H_3^+ \rightarrow C_6H_7^+ + H_2 \qquad \Delta H = -82.0\,\text{kcal mol}^{-1}. \tag{3}$$

The listed enthalpies of reaction were calculated with the B3PW91/6-311++G(2d,2p) method. Electron impact ionization of H_2 produces H_2^+, subsequent rapid exothermic proton transfer reactions (2) and (3) produce $C_6H_7^+$. The reaction of C_6H_6 with H and the neutralization reaction of $C_6H_7^+$ produce C_6H_7.

Normal H_2 (99.9999%, Scott Specialty Gases) was passed through a trap at 77 K before entering the p-H_2 converter that comprised a copper cell filled with iron (III) oxide catalyst (Aldrich) and cooled with a closed-cycle refrigerator (Advanced Research Systems, DE204AF). The efficiency of conversion was controlled by the temperature of the catalyst—typically approximately 13 K which gives a proportion of o-H_2 of less than 100 ppm. C_6H_6 (99.8%, Aldrich) and C_6D_6 (isotopic purity ~99%, Cambridge Isotope Laboratories) were used without further purification.

III. THEORETICAL CALCULATIONS

The energies, equilibrium structures, vibrational wavenumbers, and IR intensities were calculated using the GAUSSIAN 09 program.[44] Density-functional theory for calculations were performed using the B3PW91 method which uses Becke's three-parameter hybrid exchange functionals,[45]

and a correlation functional of Perdew and Wang exchange functional[46] were conducted. The standard basis set, 6-311++G(2d,2p), was used. Analytic first derivatives were utilized in geometry optimization, and anharmonic vibrational wavenumbers were calculated analytically at each stationary point. Geometric parameters of *c*-C_6H_7 and $C_6H_7^+$ predicted with various methods, vibrational displacement vectors of $C_6H_7^+$ predicted with the B3PW91/6-311++G(2d,2p) method are available from the supplementary material.[47]

IV. RESULTS

A partial IR spectra of a C_6H_6/p-H_2 (1/1000) matrix and a C_6H_6/p-H_2 (1/1000) matrix bombarded with an e-gun emitting electrons with energy of 250 eV during deposition are shown in Figs. 3(a) and 3(b), respectively, for the spectral ranges 750−1320 cm^{-1}. Many new features appear in Fig. 3(b). To differentiate these features, we performed secondary photolysis at various wavelengths and identified lines in each group according to their correlations in intensity variations. The resultant difference spectrum upon photolysis at 365 nm for 2 h with a light-emitting diode is shown in Fig. 3(c). The difference spectrum was obtained on subtraction of the spectrum recorded before irradiation from that recorded after irradiation; lines pointing upward indicate production, whereas those pointing downward indicate destruction. Irradiation of the matrix at 365 nm is expected to release electrons trapped in the matrix and to neutralize the cations. In some experiments we kept the matrix in the dark for 8−12 h and observed a difference spectrum similar to that recorded upon 365-nm irradiation but with smaller changes in line intensities; presumably some electrons can recombine with the cations slowly in the dark.

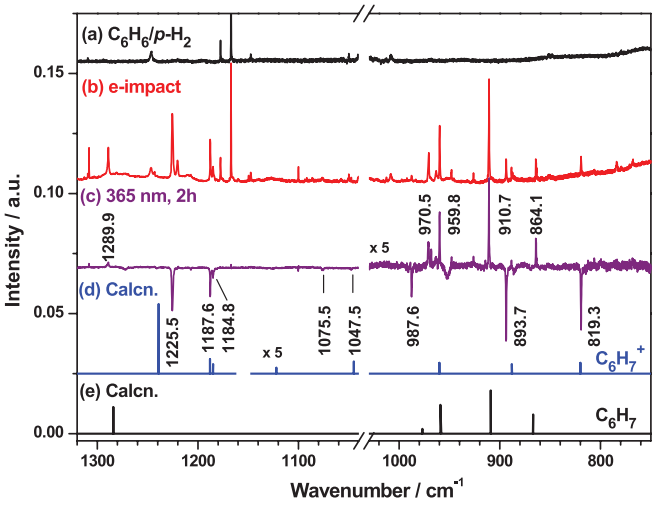

FIG. 3. Partial IR absorption spectra of matrix samples in regions 750−1320 cm^{-1}. (a) C_6H_6/p-H_2 (1/1000) deposited at 3.2 K, (b) C_6H_6/p-H_2 (1/1000) with electron bombardment during deposition at 3.2 K, (c) difference spectrum of the sample in (b) upon irradiation at 365 nm for 2 h; the intense absorption line of C_6H_6 near 1037 cm^{-1} has been removed, (d) stick spectrum of $C_6H_7^+$ simulated based on harmonic vibrational wavenumbers calculated with the CCSD(T*)-F12a/VDZ-F12 method and anharmonic contributions and IR intensities calculated with the B2PLYP-D/VTZ method,[24] and (e) stick spectrum of C_6H_7 simulated based on anharmonic vibrational wavenumbers and IR intensities calculated with the B3PW91/6-311++G(2d,2p) method.

TABLE I. Comparison of experimental vibrational wavenumbers (in cm^{-1}) of *c*-C_6H_7.

Mode	Symmetry	LIF/gas	IR/Xe	IR/*p*-H_2
ν_1	a_1			3080.4 (13)[a]
ν_2	a_1			3030.5 (3)
ν_3	a_1			3050.0 (10)
ν_4	a_1		2768	2780.1 (23)
ν_5	a_1	1571		
ν_6	a_1			1425.6 (5)
ν_7	a_1		1387	1394.7 (9)
ν_8	a_1	1174		
ν_{10}	a_1	981	958	959.8 (5)
ν_{11}	a_1			864.1 (3)
ν_{12}	a_1	559		
ν_{16}	a_2	375		
ν_{17}	b_1			2757.4 (10)
ν_{18}	b_1			970.5 (1)
ν_{19}	b_1		908	910.7 (7)
ν_{21}	b_1		618/620	622.0 (100)
ν_{22}	b_1		546	510.2 (11)
ν_{24}	b_2			3056.8? (14)[b]
ν_{27}	b_2			1389.7 (1)
ν_{29}	b_2		1287	1289.9 (4)
ν_{33}	b_2	600		
Reference		34	35	This work

[a]Relative IR intensities normalized to the most intense line (ν_{21}) of *c*-C_6H_7 are listed in parentheses.
[b]The ? mark indicates that the assignment is tentative.

As shown in Fig. 3(c), lines at 864.1, 910.7, 959.8, 970.5, and 1289.9 cm^{-1} increased in intensity upon UV irradiation. These features, demonstrating a correlated change in intensity at various stages of experiments and in separate experiments, are designated as group A. A complete list of lines in group A is shown in Table I. These lines might be assigned to absorption of cyclohexadienyl (*c*-C_6H_7) radical because a majority of intense lines observed in this work correspond well with those reported previously for *c*-C_6H_7 in a Xe matrix, as compared in Table I.[35] The broad feature near 950 cm^{-1} in Fig. 3(c) is an artifact from the subtraction.

The features pointing downward at 819.3, 893.7, 987.6, 1047.5, 1075.5, 1184.8, 1187.6, and 1225.5 cm^{-1}, shown in Fig. 3(c), also demonstrate a correlated change in intensity at various stages of experiments and in separate experiments. These features are designated as group B and assigned to $C_6H_7^+$, as discussed in Sec. V B; a complete list is summarized in Table II.

Experiments on electron bombardment of a mixture of C_6D_6/p-H_2 (1/1000) were performed to provide more information on the assignments of IR features in groups A and B. Similar experimental procedures were followed, and a representative difference IR spectrum in ranges of 700−1500 and 2650−2840 cm^{-1} upon irradiation at 365 nm is depicted in Fig. 4(a). Lines indicated with * are due to residues from subtraction of intense lines of C_6D_6. The features pointing upward and indicated with wavenumbers 748.2, 758.1, 797.6, 831.3, 1237.8, 1246.1, 1247.7, and 2784.1 cm^{-1} belong to group A. A complete list of lines in group A observed in the

TABLE II. Wavenumbers (in cm^{-1}) and IR intensities of experimental results compared with theoretical predictions for $C_6H_7^+$ and $C_6H_7^+$-Ar.

		$C_6H_7^+$			$C_6H_7^+$-Ar
Mode[a]	Sym.	Calculation[b]	IRMPD[c]	p-H_2[d]	IRPD[c]
ν_1	a_1	3081 (1)[e]			
ν_{24}	b_2	3105 (4)			3107
ν_2	a_1	3083 (3)			3078
ν_{25}	b_2	3067 (2)			
ν_4	a_1	2813 (35)		2813.1 (22)[e]	2820
ν_{17}	b_1	2808 (13)		2798.5 (11)	2809
ν_5	a_1	1590 (36)		1603.4 (27)	1607
ν_{27}	b_2	1452 (100)	1433	1451.9 (100)	1456
ν_6	a_1	1446 (13)		1445.2 (8)	
ν_{29}	b_2	1338 (8)		1328.1? (7)	1334
ν_7	a_1	1239 (58)	1228	1225.5 (55)	1239
ν_8	a_1	1188 (12)		1187.6 (21)	1198
ν_{30}	b_2	1185 (8)		1184.8 (10)	
ν_{31}	b_2	1122 (1)		1075.5? (4)	
ν_{18}	b_1	1045 (2)		1047.5? (1)	1058
ν_{32}	b_2	960 (9)		987.6 (6)	964
ν_{11}	a_1	888 (8)		893.7 (10)	903
ν_{20}	b_1	820 (9)		819.3 (9)	831
ν_{21}	b_1	640 (29)		640.8 (21)	
ν_{33}	b_2	573 (3)		576.8 (3)	
Reference		24	22	This work	23

[a]Weak (intensity < 1 km mol^{-1}) or inactive IR modes are unlisted.
[b]Harmonic vibrational wavenumbers calculated with CCSD(T*)-F12a/VDZ-F12 including anharmonic contributions calculated with B2PLYP-D/VTZ.
[c]IRMPD: Infrared multiphoton dissociation; IRPD: infrared photodissociation.
[d]The ? mark indicates that the assignment is tentative.
[e]Relative IR intensities normalized to the 194 km mol^{-1} value predicted for the most intense line for $C_6H_7^+$ at 1452 cm^{-1} with the B2PLYP-D/VTZ method.

C_6D_6/p-H_2 (1/1000) experiments is shown in Table III. The features pointing downward and indicated with wavenumbers 773.0, 865.6, 908.2, 953.0, 1076.1, 1272.8, 1306.6, 1430.7, and 2792.8 cm^{-1} in Fig. 4(a) belong to group B. A complete list of lines in group B observed in the C_6D_6/p-H_2 (1/1000) experiments is shown in Table IV.

Cordonnier *et al.* reported that, in p-H_2 plasma, the electron impact ionization followed by the ion-neutral reaction, reaction (2), produces pure p-H_3^+, but the subsequent reactions between p-H_3^+ and p-H_2 scrambles protons; the hydrogen exchange reaction produces o-H_3^+ and acts as the gateway for nuclear spin conversion.[48] We did observe weak absorption features of $Q_1(0)$ of H_2 near 4153 cm^{-1} induced by presence of o-H_2 and the $Q_1(1) + S_0(1)$ band near 4750 cm^{-1}, indicating that a small yield for conversion to o-H_2 in our experiments.

V. DISCUSSION

A. Assignment of lines in group A to *c*-C_6H_7

Lines in group A, shown as positive features in Fig. 3(c), increased in intensity upon UV irradiation. Because irradiation of the matrix at 365 nm is expected to release electrons trapped in the matrix and to neutralize the cations, it is thus expected that lines in group A are associated with a neutral species and those in group B are associated with a cation.

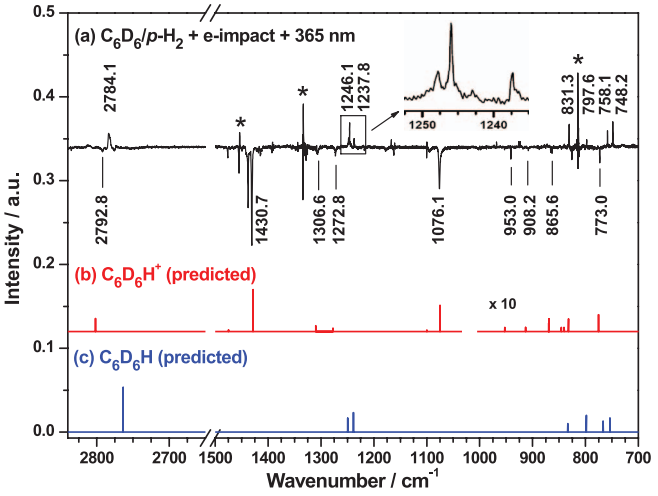

FIG. 4. Partial IR absorption spectra of matrix samples in regions 700−1500 and 2650−2840 cm^{-1}. (a) Difference spectrum of the electron-bombarded C_6D_6/p-H_2 (1/1000) sample upon irradiation at 365 nm for 2 h, (b) stick spectrum of $C_6D_6H^+$, and (c) stick spectrum of c-C_6D_6H simulated based on anharmonic vibrational wavenumbers and IR intensities calculated with the B3PW91/6-311++G(2d,2p) method. Lines indicated with * are due to residues from subtraction of intense lines of C_6D_6.

Lines in group A are readily assigned to absorption of cyclohexadienyl (c-C_6H_7) radical according to comparison with lines previously observed in a Xe matrix.[35] (Table I) and vibrational wavenumbers and relative IR intensities predicted quantum-chemically, as listed in Table III.

Seven vibrational modes with lines at 2768, 1387, 1287, 958, 908, 618/620, and 546 cm^{-1} were reported for c-C_6H_7 isolated in a Xe matrix. Except the one at 546 cm^{-1}, these features are close to the corresponding lines at 2780.1, 1394.7, 1289.9, 959.8, 910.7, and 622.0 cm^{-1} observed in our experiments. We did not observe any line near 546 cm^{-1}; the closest line was observed at 510.2 cm^{-1}. The additional lines at 864.1 and 970.5 cm^{-1} in Fig. 3(c) were unobserved in the Xe matrix, probably because they are weaker than lines at 959.8 and 910.7 cm^{-1}. We observed in total 16 lines that can be assigned to c-C_6H_7, much more than the 7 lines reported for c-C_6H_7 in the Xe matrix. Lines reported in the Xe matrix are associated with the more intense lines observed in this work.

Observed lines agree with anharmonic vibrational wavenumbers predicted with the B3PW91/6-311++G(2d,2p) method, as shown in Figs. 3(c) and 3(e) and listed in Table III. The deviations in wavenumbers less than 0.7% except ν_{24} which was tentatively assigned to a feature at 3056.8 cm^{-1} and shows a deviation of 1.0%. Observed relative IR intensities also agree satisfactorily with the predicted values, except those of C−H stretching modes (ν_4, ν_{17}, and ν_{24}) which are 2−3 times weaker than predicted. Because of the narrow spectral widths and superb sensitivity of this method, nearly all lines with predicted intensities greater than 1 km mol^{-1} were identified.

The C_6D_6/p-H_2 experiments provide further support for the assignment and lines in group A observed in the C_6D_6/p-H_2 experiments are assigned to c-C_6D_6H. In Fig. 4(a) the upward-pointing lines in group A are at 748.2, 758.1, 797.6, 831.3, 1237.8, 1246.1, 1247.7, and 2784.1 cm^{-1}, consistent

TABLE III. Comparison of observed and theoretical vibrational wavenumbers (in cm^{-1}) and relative IR intensities of c-C_6H_7 and c-C_6D_6H.

	c-C_6H_7		c-C_6D_6H		
Mode	Theory[a]	p-H_2[b]	Theory[a]	p-H_2[b]	Isotopic ratio[c]
ν_1 (a_1)	3071 (14)[d]	3080.4 (13)[d]	2292 (10)[d]	2297.7 (12)[e]	0.7459 (0.7464)
ν_2 (a_1)	3035 (4)	3030.5 (3)	2273 (8)		
ν_3 (a_1)	3049 (9)	3050.0 (10)	2241 (5)	2232.3 (13)	0.7319 (0.7349)
ν_4 (a_1)	2763 (52)	2780.1 (23)	2764 (68)	2784.1 (68)	1.0014 (1.0002)
ν_5 (a_1)	1564 (0)		1529 (0)		
ν_6 (a_1)	1424 (5)	1425.6 (5)	1239 (3)	1237.8 (6)	0.8683 (0.8700)
ν_7 (a_1)	1405 (8)	1394.7 (9)	1239 (18)	1246.1 (19)	0.8935 (0.8823)
ν_8 (a_1)	1177 (0)		897 (0)		
ν_9 (a_1)	981 (0)		953 (0)		
ν_{10} (a_1)	959 (6)	959.8 (5)	798 (15)	797.6 (8)	0.8310 (0.8324)
ν_{11} (a_1)	867 (4)	864.1 (3)	754 (13)	748.2 (16)	0.8659 (0.8706)
ν_{12} (a_1)	558 (0)		535 (0)		
ν_{13} (a_2)	1151 (0)		842 (1)		
ν_{14} (a_2)	959 (0)		757 (0)		
ν_{15} (a_2)	721 (0)		555 (0)		
ν_{16} (a_2)	375 (0)		331 (0)		
ν_{17} (b_1)	2755 (20)	2757.4 (10)	2041 (35)	2041.4 (8)	0.7403 (0.7407)
ν_{18} (b_1)	977 (1)	970.5 (1)	836 (3)	840.0?(1)	0.8655 (0.8566)
ν_{19} (b_1)	909 (9)	910.7 (7)	834 (8)	831.3 (18)	0.9128 (0.9169)
ν_{20} (b_1)	965 (0)		767 (10)	758.1 (13)	
ν_{21} (b_1)	625 (100)	622.0 (100)	463 (100)	461.6 (100?)	0.7421 (0.7398)
ν_{22} (b_1)	518 (12)	510.2 (11)	437 (38)		
ν_{23} (b_1)	173 (0)		149 (0)		
ν_{24} (b_2)	3030 (51)	3056.8? (14)	2269 (50)	2267.2 (20)	0.7417 (0.7490)
ν_{25} (b_2)	3041 (2)		2250 (3)	2246.9 (7)	
ν_{26} (b_2)	1510 (1)		1431 (0)		
ν_{27} (b_2)	1387 (1)	1389.7 (1)	1116 (3)		
ν_{28} (b_2)	1340 (0)		1322 (0)		
ν_{29} (b_2)	1284 (8)	1289.9 (4)	1250 (13)	1247.7 (10)	0.9673 (0.9735)
ν_{30} (b_2)	1152 (0)		826 (0)		
ν_{31} (b_2)	1095 (0)		996 (0)		
ν_{32} (b_2)	777 (0)		625 (0)		
ν_{33} (b_2)	587 (1)		563 (3)		

[a]Anharmonic vibrational wavenumbers of c-C_6H_7 and c-C_6D_6H were calculated with the B3PW91/6-311++G(2d,2p) method.
[b]The ? mark indicates that the assignment is tentative.
[c]Defined as the ratio of wavenumber of the isotopic species to that of c-C_6H_7; theoretical values are listed in parentheses for comparison.
[d]Relative intensities listed in parentheses were normalized to the most intense band (ν_{21}) of c-C_6H_7 and c-C_6D_6H which were calculated to be 89.3 and 40.2 km mol^{-1}, respectively, with B3PW91/6-311++G(2d,2p).
[e]The ? mark indicates that the intensity could not be determined accurately due to poor signal-to-noise ratio near the wavelength limit of detection. Observed intensities are normalized to the predicted IR intensity of the second most intense line at 2784.1 cm^{-1}.

with those shown in Fig. 4(c) for theoretically predicted stick spectrum of c-C_6D_6H at 754 (ν_{11}), 767 (ν_{20}), 798 (ν_{10}), 834 (ν_{19}),1239 (ν_7), 1239 (ν_6), 1250 (ν_{29}), and 2764 (ν_4) cm^{-1} according to anharmonic vibrational wavenumbers and IR intensities calculated with the B3PW91/6-311++G(2d,2p) method. The feature due to the CH-stretching mode was observed at 2784.1 cm^{-1}, indicating that the isotopic variant of mono-hydrogenated benzene that we produced in this experiment is C_6D_6H.

Table III compares wavenumbers and relative IR intensities of all observed lines in group A in the C_6H_6/p-H_2 and C_6D_6/p-H_2 experiments with anharmonic vibrational wavenumbers and IR intensities of c-C_6H_7 and c-C_6D_6H predicted with the B3PW91/6-311++G(2d,2p) method. The agreements in wavenumbers and relative IR intensities are satisfactory. The experimental isotopic ratios agree satisfactorily with those predicted with theory, with deviations less than 0.009. Hence, we are confident with the assignment of features in group A to c-C_6H_7 and c-C_6D_6H in experiments of C_6H_6/p-H_2 and C_6D_6/p-H_2, respectively.

As shown in Table I, most vibrational modes reported previously from experiments on laser-induced fluorescence[34] do not match with modes observed in IR, even though they correspond well to predicted values of vibrational modes which are IR inactive. It is unclear if these bands observed in laser-induced fluorescence were misassigned or the Franck-Condon active modes are different from the IR active modes. Further investigations are desired.

B. Assignment of lines in group B to $C_6H_7^+$

The observation of the decay of these features in group B and the increase of those of in group A (c-C_6H_7) implies that the neutralization took place when the matrix sample was

TABLE IV. Comparison of observed and theoretical vibrational wavenumbers (in cm^{-1}) and relative IR intensities of $C_6H_7^+$ and $C_6D_6H^+$.

	$C_6H_7^+$		$C_6D_6H^+$		
Mode	Theory[a]	p-H_2[c]	Theory[a]	p-H_2[c]	Isotopic ratio[d]
ν_1 (a_1)	3094 (1)[b]		2318 (1)[b]		
ν_2 (a_1)	3095 (3)		2285 (0)		
ν_3 (a_1)	3087 (0)		2275 (1)	2278.0? (2)[b]	
ν_4 (a_1)	2823 (38)	2813.1 (22)[b]	2802 (32)	2792.8 (7)	0.9928 (0.9927)
ν_5 (a_1)	1610 (41)	1603.4 (27)	1570 (55)	1567.1 (35)	0.9774 (0.9753)
ν_6 (a_1)	1455 (15)	1445.2 (8)	1278 (8)	1272.8 (10)	0.8807 (0.8778)
ν_7 (a_1)	1225 (63)	1225.5 (55)	1075 (62)	1076.1 (77)	0.8781 (0.8779)
ν_8 (a_1)	1196 (15)	1187.6 (21)	869 (3)	863.1 (3)	0.7268 (0.7267)
ν_9 (a_1)	1005 (0)		913 (1)	908.2? (1)	
ν_{10} (a_1)	983 (0)		953 (1)	953.0 (1)	
ν_{11} (a_1)	899 (8)	893.7 (10)	775 (4)	773.0 (6)	0.8649 (0.8621)
ν_{12} (a_1)	588 (0)		564 (0)		
ν_{13} (a_2)	1106 (0)		996 (0)		
ν_{14} (a_2)	994 (0)		751 (2)		
ν_{15} (a_2)	801 (0)		615 (0)		
ν_{16} (a_2)	321 (0)		279 (0)		
ν_{17} (b_1)	2808 (16)	2798.5 (11)	2093 (18)	2093.6 (7)	0.7481 (0.7454)
ν_{18} (b_1)	1040 (1)	1047.5? (1)	846 (1)	852.6 (<1)	0.8139 (0.8131)
ν_{19} (b_1)	1027 (0)		884 (1)	887.3? (1)	
ν_{20} (b_1)	823 (9)	819.3 (9)	679 (2)	677.2 (4)	0.8266 (0.8247)
ν_{21} (b_1)	648 (30)	640.8 (21)	497 (18)	492.0 (10)	0.7678 (0.7659)
ν_{22} (b_1)	394 (1)		342 (1)		
ν_{23} (b_1)	219 (8)		183 (6)		
ν_{24} (b_2)	3111 (4)		2305 (1)	2295.6? (6)	
ν_{25} (b_2)	3074 (2)		2283 (0)		
ν_{26} (b_2)	1583 (0)		1475 (5)	1476.3 (6)	
ν_{27} (b_2)	1457 (100)	1451.9 (100)	1429 (100)	1430.7 (100)	0.9854 (0.9805)
ν_{28} (b_2)	1401 (0)		1310 (15)	1306.6 (12)	
ν_{29} (b_2)	1339 (8)	1328.1? (7)	1100 (3)	1095.1 (12)	0.8246 (0.8211)
ν_{30} (b_2)	1193 (8)	1184.8 (10)	869 (2)	865.6 (3)	0.7306 (0.7287)
ν_{31} (b_2)	1128 (0)	1075.5? (4)	840 (3)		
ν_{32} (b_2)	971 (10)	987.6 (6)	832 (2)	845.3 (1)	0.8559 (0.8572)
ν_{33} (b_2)	582 (3)	576.8 (3)	557 (3)	552.2 (4)	0.9574 (0.9582)

[a]Anharmonic vibrational wavenumbers of $C_6H_7^+$ and $C_6D_6H^+$ were calculated with the B3PW91/6-311++G(2d,2p) method.
[b]Relative intensities listed in parentheses were normalized to the most intense band (ν_{27}) of $C_6H_7^+$ and $C_6D_6H^+$ which were calculated to be 182.6 and 163.6 km mol^{-1}, respectively, with B3PW91/6-311++G(2d,2p).
[c]The ? mark indicates that the assignment is tentative.
[d]Defined as the ratio of wavenumber of the isotopic species to that of $C_6H_7^+$; theoretical values are listed in parentheses for comparison.

maintained in the dark for an extended period or irradiated at 365 nm to release the trapped electrons; hence the carrier of these lines is most likely the corresponding cation, $C_6H_7^+$.

Observed downward lines at 819.3, 893.7, 987.6, 1047.5, 1184.8, 1187.6, and 1225.5 cm^{-1}, shown in Fig. 3(c), are consistent with corresponding anharmonic wavenumbers reported by Botschwina and Oswald[24] at 820, 888, 960, 1045, 1185, 1188, and 1239 cm^{-1}, shown in Fig. 3(d); the weak line observed at 1075.5 cm^{-1} deviates from the predicted value of 1122 cm^{-1} by 4.1%. These observed line positions are also close to those reported for C_6H_6-Ar at 831, 903, 964, and 1058 cm^{-1},[23] with deviations 4−13 cm^{-1} (<1.2%).

As listed in Table II, the wavenumbers of all observed features in group B are consistent with the anharmonic vibrational wavenumbers predicted based on harmonic vibrational wavenumbers calculated with the CCSD(T*)-F12a/VDZ-F12 method and anharmonic contributions and IR intensities calculated with the B2PLYP-D/VTZ method.[24] They are also compared in Table II with those of $C_6H_7^+$ recorded with the IRMPD method[22] and those of $C_6H_7^+$-Ar recorded with the IRPD method.[23] Observed wavenumbers and relative IR intensities of $C_6H_7^+$ agree with those calculated theoretically, with deviations in wavenumbers less than 1.1% except ν_{32} which shows a deviation of 2.9%. A stripped spectrum of $C_6H_7^+$, derived on subtraction of the absorption spectrum of C_6H_6 and c-C_6H_7 from the spectrum recorded after electron impact such that most lines due to C_6H_6 and c-C_6H_7 are removed, is shown in Fig. 2(d) and compared with the IRPD spectrum of $C_6H_7^+$-Ar in Fig. 2(b) and the stick spectrum showing quantum-chemically predicted anharmonic vibrational wavenumbers in Fig. 2(c).[24] Compared with the IRPD spectrum of $C_6H_7^+$-Ar, our IR spectrum of $C_6H_7^+$ in solid p-H_2 shows much narrower lines, with most lines having widths < 0.8 cm^{-1}, so that closely spaced lines such as those at 1184.8 and 1187.6 cm^{-1} are resolved, as shown in the inset of Fig. 2; these close-lying lines are also predicted

by theory at 1185 and 1188 cm^{-1},[24] as listed in Table II. The much broader spectral coverage of the Fourier-transform IR spectrometer also enables us to observe lines at 576.8 and 640.8 cm^{-1} that were unreported in the IRPD experiments;[23] the latter line carries significant intensity. Furthermore, our spectrum presents true IR intensities that are in satisfactory agreement with theoretical predictions; lines in the C−H stretching region are much weaker than those observed with the Ar-tagging IRPD method.

Experiments on C_6D_6/*p*-H_2 provide further support for the assignments. In order to understand the deuterium isotopic shifts, we performed calculations on both $C_6H_7^+$ and $C_6D_6H^+$ with the B3PW91/6-311++G(2d,2p) method to predict IR intensities and anharmonic vibrational wavenumbers, as listed in Table IV. As shown in Fig. 4, experimental lines pointing downward (trace a) are compared with the stick spectrum of $C_6D_6H^+$ predicted with the B3PW91/6-311++G(2d,2p) method (trace b). Observed lines at 773.0, 865.6, 908.2, 953.0, 1076.1, 1272.8, 1306.6, 1430.7, and 2792.8 cm^{-1} are consistent with anharmonic vibrational wavenumbers predicted at 775, 869, 913, 953, 1075, 1278, 1310, 1249, and 2802 cm^{-1} for $C_6D_6H^+$. The weak feature observed at 2792.8 cm^{-1} due to the CH-stretching mode supports that the isotopic variant of protonated benzene that we produced in this experiment is $C_6D_6H^+$.

Lists of observed wavenumbers and relative IR intensities of all lines in group B from experiments of C_6H_6/*p*-H_2 and C_6D_6/*p*-H_2 are compared in Table IV with anharmonic vibrational wavenumbers and IR intensities of $C_6H_7^+$ and $C_6D_6H^+$ predicted with the B3PW91 method, respectively. The experimental isotopic ratios agree satisfactorily with those predicted with theory, with deviations less than 0.005. Observed relative IR intensities also agree satisfactorily with theoretical predictions. Hence, we are confident with the assignment of features in group B to $C_6H_7^+$ and $C_6D_6H^+$ in experiments of C_6H_6/*p*-H_2 and C_6D_6/*p*-H_2, respectively.

The deuterium isotopic experiments clearly support the mechanism that, upon electron bombardment of H_2, H_3^+ was produced and a proton was transferred from H_3^+ to C_6H_6 (or C_6D_6) to form $C_6H_7^+$ (or $C_6D_6H^+$); *c*-C_6H_7 (or *c*-C_6D_6H) radicals are also produced from neutralization of $C_6H_7^+$ (or $C_6D_6H^+$) or reaction of H with C_6H_6 (or C_6D_6). As evidenced by the fact that *c*-C_6H_7 and $C_6H_7^+$ are the only major products observed in this experiment, we think that this is a much "cleaner" method to produce protonated aromatic hydrocarbons and its neutral species.

Although the Ar-tagging IRPD method seems to provide better spectra than IRMPD, the observed features are still broad. Moreover, a critical limitation of the Ar-tagging method is its difficulty in tagging a larger protonated PAH because of its large internal energy; so far the largest protonated PAH detected with this method is protonated naphthalene.[49] According to an astrochemical model, PAH molecules containing 20–80 carbon atoms are photochemically more stable in interstellar clouds.[50] The similarity between the IRMPD spectrum of protonated coronene ($C_{24}H_{12}$) and the UIE spectrum indicate that protonated coronene and higher PAH might contribute to the UIE bands.[51] IR spectra of protonated coronene and higher PAH with improved resolution and spectral coverage are thus desirable. Our preliminary results indicate that this technique is also applicable to protonated coronene.

VI. CONCLUSION

Electron bombardment was applied during deposition of a mixture of C_6H_6 and an excess of *p*-H_2 at 3.2 K to generate *c*-C_6H_7 and $C_6H_7^+$ in the *p*-H_2 matrix. Lines of *c*-C_6H_7 increased in intensity upon irradiation of the matrix at 365 nm, whereas those of $C_6H_7^+$ decreased in intensity. Observed vibrational wavenumbers and relative IR intensities of these lines agree well with those of *c*-C_6H_7 and $C_6H_7^+$ predicted by theory. Our spectrum of *c*-C_6H_7 provides twice more lines than previous report for *c*-C_6H_7 in a Xe matrix. Our spectrum of $C_6H_7^+$ extended the spectral limit from 800 cm^{-1} to 550 cm^{-1} and presents true IR intensities that are in satisfactory agreement with theoretical predictions; line intensities in the C−H stretching region of $C_6H_7^+$ observed with the Ar-tagging IRPD method region are much larger than theoretical predictions. The IR lines of $C_6H_7^+$ exhibit narrow widths so that closely spaced lines are resolved.

Our results clearly indicate that *c*-C_6H_7 and $C_6H_7^+$ are the major products and their IR spectra with much improved resolution, signal-to-noise ratio, and spectral coverage were recorded. This "clean" method provides a direct IR characterization of the protonated aromatic and its neutral species and will be applicable to investigate the high-resolution IR spectra of larger protonated PAH and its neutral counterpart or other organic compounds[52] that are postulated as carriers of unidentified infrared emission bands in the interstellar media.

ACKNOWLEDGMENTS

National Science Council in Taiwan supported this work under the Contract No. NSC100-2745-M-009-001-ASP. Y.J.W. thanks support from Beamline 14A at National Synchrotron Radiation Research Center (NSRRC) in Taiwan. The National Center for High-Performance Computing provided computer time.

[1] J. March, *Advanced Organic Chemistry: Reactions, Mechanisms, and Structure* (McGraw Hill, New York, 1977).
[2] T. P. Snow, V. Le Page, Y. Keheyan, and V. M. Bierbaum, Nature (London) **391**, 259 (1998).
[3] A. L. Sobolewski, W. Domcke, C. Dedonder-Lardeux, and C. Jouvet, Phys. Chem. Chem. Phys. **4**, 1093 (2002).
[4] O. V. Boyarkin, S. R. Mercier, A. Kamariotis, and T. R. Rizzo, J. Am. Chem. Soc. **128**, 2816 (2006).
[5] G. A. Olah, J. S. Staral, G. Asencio, G., Liang, D. A. Forsyth, and G. D. Mateescu, J. Am. Chem. Soc. **100**, 6299 (1978).
[6] V. A. Koptyug and C. Rees, Top. Curr. Chem. **122**, 1 (1984).
[7] D. Kuck, Angew. Chem. Int. Ed. **39**, 125 (2000).
[8] T. Xu, D. H. Barich, P. D. Torres, and J. F. Haw, J. Am. Chem. Soc. **119**, 406 (1997).
[9] S.-L. Chong and J. L. Franklin, J. Am. Chem. Soc. **94**, 6630 (1972).
[10] J. E. Szulejko and T. B. McMahon, J. Am. Chem. Soc. **115**, 7839 (1993).
[11] E. P. Hunter and S. G. Lias, J. Phys. Chem. Ref. Data **27**, 413 (1998).
[12] W. J. Hehre and J. A. Pople, J. Am. Chem. Soc. **94**, 6901 (1972).
[13] R. S. Mason, C. M. Williams, and P. D. J. Anderson, J. Chem. Soc. Chem. Commun. **1995**, 1027.
[14] M. Li, M. Lin, and A. M. Rustum, Rapid Commun. Mass Spectrom. **24**, 1707 (2010).

[15]H.-H. Perkampus and E. Baumgarten, Angew. Chem. Int. Ed. **3**, 776 (1964).
[16]B. S. Freiser and J. L. Beauchamp, J. Am. Chem. Soc. **98**, 3136 (1976).
[17]Y. Okami, N. Nanbu, S. Okuda, S. Hamanaka, and M. Ogawa, Tetrahedron Lett. **13**, 5259 (1972).
[18]C. A. Reed, N. L. P. Fackler, K.-C. Kim, D. Stasko, and D. R. Evans, J. Am. Chem. Soc. **121**, 6314 (1999).
[19]I. Garkusha, J. Fulara, A. Nagy, and J. P. Maier, J. Am. Chem. Soc. **132**, 14979 (2010).
[20]N. Solcá and O. Dopfer, Angew. Chem. Int. Ed. **41**, 3628 (2002).
[21]N. Solcá and O. Dopfer, Chem. Eur. J. **9**, 3154 (2003).
[22]W. Jones, P. Boissel, B. Chiavarino, M. E. Crestoni, S. Fornarini, J. Lemaire, and P. Maitre, Angew. Chem. Int. Ed. **42**, 2057 (2003).
[23]G. E. Douberly, A. M. Ricks, P. v. R. Schlever, and M. A. Duncan, J. Phys. Chem. A **112**, 4869 (2008).
[24]P. Botschwina and R. Oswald, J. Phys. Chem. A **115**, 13664 (2011).
[25]T. Shida and W. H. Hamill, J. Am. Chem. Soc. **88**, 3689 (1966).
[26]T. Shida and I. Hanazaki, Bull. Chem. Soc. Jpn. **43**, 646 (1970).
[27]T. Shida and I. Hanazaki, J. Phys. Chem. **74**, 213 (1970).
[28]J. H. Miller, L. Andrews, P. A. Lund, and P. N. Schatz, J. Chem. Phys. **73**, 4932 (1980).
[29]T. Shida, J. Chem. Phys. **64**, 2703 (1976).
[30]S. J. Sheng, J. Phys. Chem. **82**, 442 (1978).
[31]F. Berho, M.-T. Rayez, and R. Lesclaux, J. Phys. Chem. A **103**, 5501 (1999).
[32]F. Berho and R. Lesclaux, Phys. Chem. Chem. Phys. **3**, 970 (2001).
[33]E. Estupinan, E. Villenave, S. Raoult, J. C. Rayez, M. T. Rayez, and R. Lesclaux, Phys. Chem. Chem. Phys. **5**, 4840 (2003).
[34]T. Imamura, W. Zhang, H. Horiuchi, H. Hiratsuka, T. Kudo, and K. Obi, J. Chem. Phys. **121**, 6861 (2004).
[35]V. I. Feldman, F. F. Sukhov, E. A. Logacheva, A. Y. Orlov, I. V. Tyulpina, and D. A. Tyurin, Chem. Phys. Lett. **437**, 207 (2007).
[36]T. Oka, Annu. Rev. Phys. Chem. **44**, 299 (1993).
[37]T. Momose and T. Shida, Bull. Chem. Soc. Jpn. **71**, 1 (1998).
[38]K. Yoshioka and D. T. Anderson, J. Chem. Phys. **119**, 4731 (2003).
[39]M. Bahou, and Y.-P. Lee, J. Chem. Phys. **133**, 164316 (2010).
[40]J. Amicangelo and Y.-P. Lee, J. Phys. Chem. Lett. **1**, 2956 (2010).
[41]Y.-F. Lee and Y.-P. Lee, J. Chem. Phys. **134**, 124314 (2011).
[42]Y.-P. Lee, Y.-J. Wu, R. M. Lees, L.-H. Xu, and J. T. Hougen, Science **311**, 365 (2006).
[43]Y.-P. Lee, Y.-J. Wu, and J. T. Hougen, J. Chem. Phys. **129**, 104502 (2008)
[44]M. J. Frisch, G. W. Trucks, H. B. Schlegel *et al.*, GAUSSIAN 09, Revision A.02, Gaussian, Inc., Wallingford, CT, 2009.
[45]A. D. Becke, J. Chem. Phys. **98**, 5648 (1993).
[46]J. P. Perdew, K. Burke, and Y. Wang, Phys. Rev. B **54**, 16533 (1996).
[47]See supplementary material at http://dx.doi.org/10.1063/1.3703502 for geometric parameters of *c*-C_6H_7 and $C_6H_7^+$ predicted with various methods and vibrational displacement vectors of $C_6H_7^+$.
[48]M. Cordonnier, D. Uy, R. M. Dickson, K. E. Kerr, Y. Zhang, and T. Oka, J. Chem. Phys. **113**, 3181 (2000).
[49]A. M. Ricks, G. E. Douberly, and M. A. Duncan, Astrophys. J. **702**, 301 (2009).
[50]A. G. G. M. Tielens, Ann. Rev. Astron. Astronphys. **46**, 289 (2008).
[51]H. Knorke, J. Langer, J. Oomens, and O. Dopfer, Astrophys. J. Lett. **706**, L66 (2009).
[52]S. Kwok and Y. Zhang, Nature (London) **479**, 80 (2011).